LC-PHSM-2005-002
9th May 2005

Selectron Production in $e\gamma$ Collisions at a Linear Collider

I. Alvarez Illan, K. Mönig
DESY, Zeuthen

Abstract

If the mass splitting between gauginos and sleptons is relatively large, it is possible that only gauginos can be seen in an e^+e^- linear collider. If the mass slitting is, however, not too large the selectron might be visible in the process $e\gamma \rightarrow \tilde{e}\tilde{\chi}_1^0$. This process is simulated for the parameters of an $e\gamma$ collider at TESLA and the precision with which the selectron mass can be measured is estimated.

1 Introduction

In supersymmetric models the mass splitting between the gauginos and the sfermions is to a large extend arbitrary. If the mass difference between the lightest neutralino and the selectron is a few hundred GeV a situation may arise where gauginos are visible e.g. in chargino production at the ILC while selectron pair production is kinematically forbidden. However the sum of the lightest neutralino and the selectron mass can still be below 90% of the centre of mass energy, so that the process $e^-\gamma \rightarrow \tilde{e}^-\tilde{\chi}_1^0$ is possible at an $e^-\gamma$ collider. This situation is studied in this note for a linear collider with 500 GeV centre of mass energy. It will be assumed that the photon collider will be run for one year with the parameters presented in [1] for the $\gamma\gamma$ collider, however with only one laser switched on. These parameters result in a total $e\gamma$ luminosity of $\mathcal{L} = 6.8 \cdot 10^{34}\mathrm{cm}^{-2}\mathrm{s}^{-1}$ integrated over the full energy spectrum corresponding to $\mathcal{L} = 2.5 \cdot 10^{34}\mathrm{cm}^{-2}\mathrm{s}^{-1}$ for $\sqrt{s(e\gamma)} > 350\mathrm{GeV}$. The present study is on generator level only. However the event selection is only based on the selection of isolated energetic electrons, so that no degradation is expected, if detector effects are taken into account.

2 Cross Sections

The simulation is made in the mSUGRA scenario with the parameters

$$\begin{aligned} A &= 0 \\ M_0 &= 250\,\mathrm{GeV} \\ M_{\frac{1}{2}} &= 250\,\mathrm{GeV} \\ \tan\beta &= 50 \\ \mathrm{sign}\mu &= + \end{aligned}$$

These parameters are chosen to fulfil the LEP constraints in Higgs and SUSY searches and at the same time give superpartner masses within the desired scenario. With these parameters the relevant masses are:

$$\begin{aligned} m(\tilde{\chi}_1^0) &= 100.3\,\mathrm{GeV} \\ m(\tilde{e}_R^-) &= 269.8\,\mathrm{GeV} \end{aligned}$$

It will be assumed that the neutralino mass will be known accurately in this scenario. The processes are generated by the computer tool SHERPA 1.0.3 [2], using a centre of mass energy of 500 GeV and an electron polarisation of 90%. The photon spectrum is simulated using CompAZ [3]. The maximum photon energy from the laser-backscattering process is around 80% of the beam energy [1]. With these values the cross sections, averaged over the full energy spectrum, are reasonably large, around 0.06 pb in the experimental setup chosen corresponding to 40000 produced selectrons per year[1]. The experimental signature is a single electron in the detector. There is a huge potential background from $e\gamma \to W\nu$ with $W \to e\nu$. This background can be efficiently suppressed by working with a right-handed electron beam. Since the lighter selectron is the partner of the right-handed electron this polarisation simultaneously enhances the signal cross section and suppresses the production of left-handed selectrons which have already a much smaller cross section because of their higher mass.

The Feynman diagrams contributing to the process under study are shown in Figure 1. The cross section depends on the $e\tilde{e}_R\tilde{\chi}^0_1$ coupling and thus on the parameters of the neutralino mixing matrix. However since this coupling appears in the same way in both diagrams, the differential distributions are independent on these parameters.

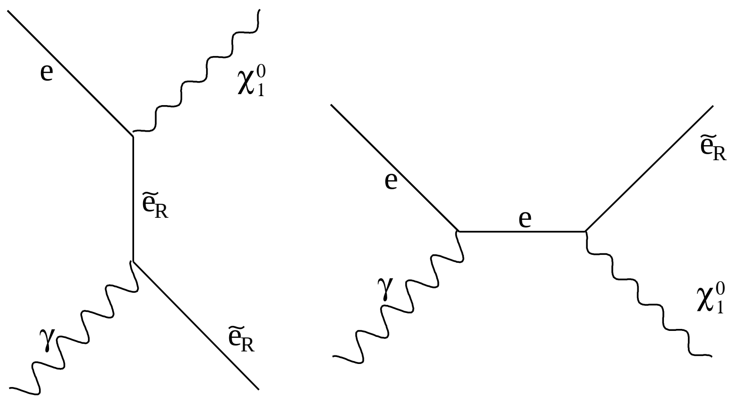

Figure 1: Feynman diagrams contributing to $e^-\gamma \to \tilde{e}^-\tilde{\chi}^0_1$.

Figure 2 shows the cross sections of the signal for the two photon polarisation states. The results of the simulation are in agreement with earlier calculations [4]. At low centre of mass energies the cross section is larger for an $e\gamma$ angular momentum of $|J| = 1/2$ which is used in the analysis. Left handed selectrons are further suppressed by this choice since they are produced from left handed electrons and thus from the $|J| = 3/2$ state. Adding the fact that about half of the left handed selectrons decay into $\nu\tilde{\chi}^\pm_1$ their cross section is at least a factor 100 smaller than the signal. They are not considered further in this note.

[1] A year is assumed to be 10^7 s at design luminosity.

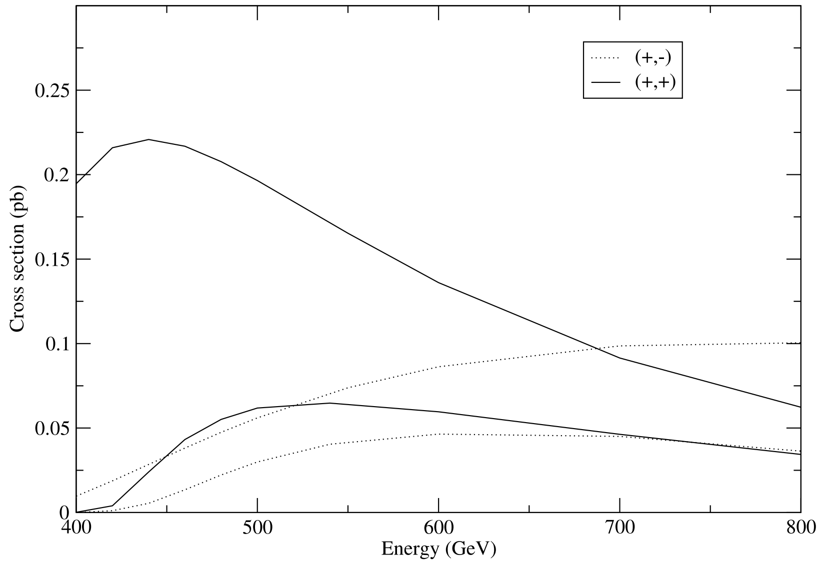

Figure 2: Cross section $e^-\gamma \to \tilde{e}^-\tilde{\chi}_1^0$ for right-handed e^- and left- $(+,-)$ and right-handed $(+,+)$ photon polarisation as a function of the centre of mass energy. The upper curves are for a fixed photon energy equal to the electron energy. The lower curves are for a realistic photon energy spectrum at a given e^-e^- centre of mass energy.

The energy and angular distribution of the signal electrons are shown in Figure 3[2]. The signal has the nice property of being homogeneous distributed in the polar angle θ.

3 Background

There are two important backgrounds to this process due to Standard Model particles, $e^-\gamma \to W^-\nu_e \to e^-\nu_e\overline{\nu_e}$ and $e^-\gamma \to Ze^- \to e^-\nu\overline{\nu}$. The cross sections of other Standard Model and SUSY backgrounds are negligible. The energy and angular distributions for the two background processes are shown in Figures 4 and 5.

Using right-handed electrons the background is reduced considerably but still, it is necessary to implement some cuts. The background is largely peaked at low polar angles. With an angular cut of $\cos\theta \leq 0.5$ and a transverse momentum cut of $P_t \leq 150\,\mathrm{GeV}$ one can obtain 71% efficiency and 63% purity, allowing for a precision on the production cross section of 0.75%. The purity can be improved further reducing the upper value of the angle cut

[2] In this note all figures are normalised to 50000 signal events.

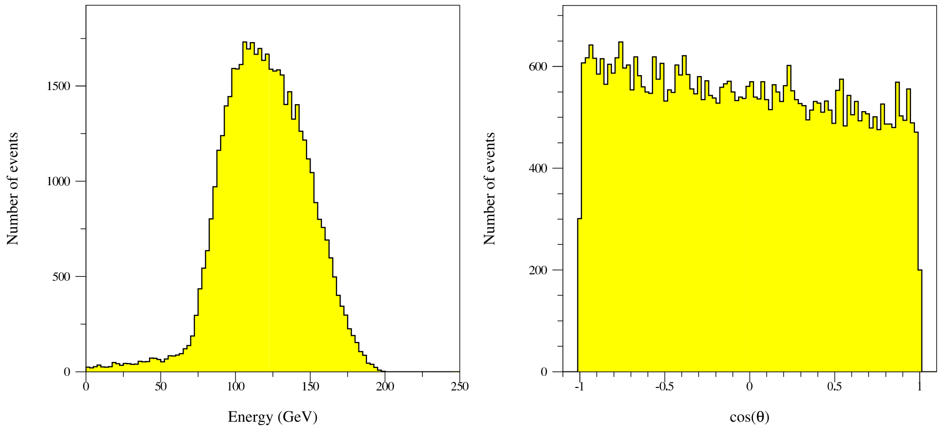

Figure 3: Energy and angular distribution of the signal electrons.

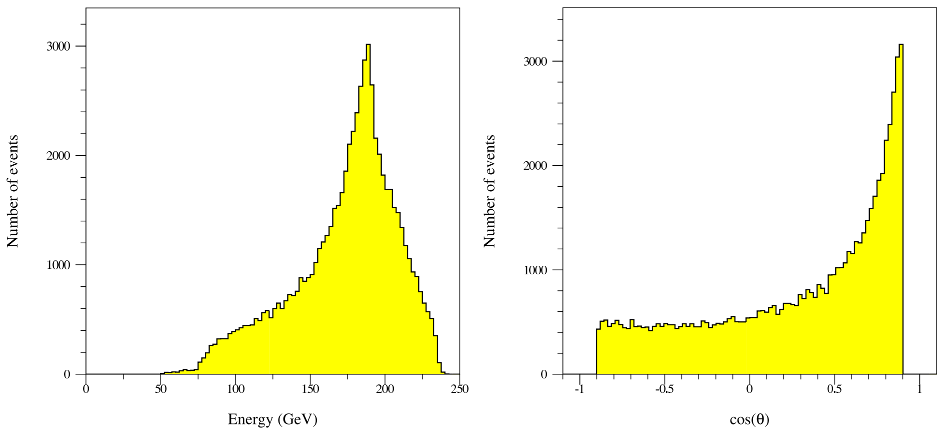

Figure 4: Energy and angular distribution for electrons from $e^-\gamma \to Ze \to e^-\nu_\mu\overline{\nu_\mu}, e^-\nu_\tau\overline{\nu_\tau}$.

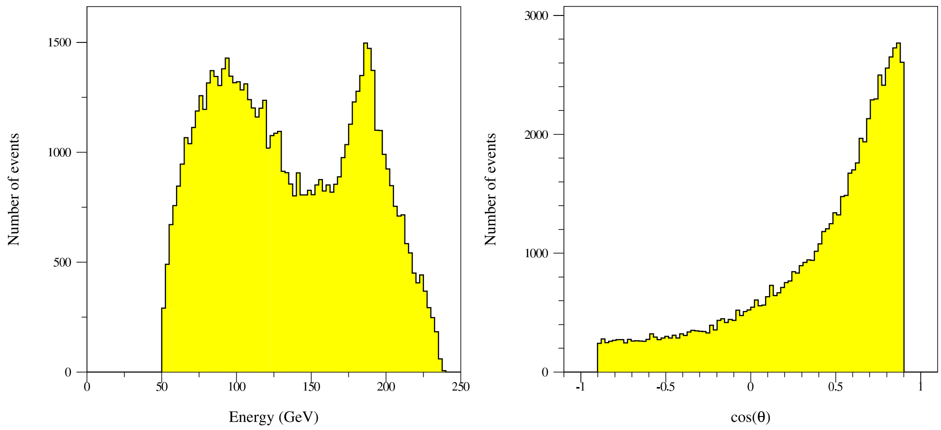

Figure 5: Energy and angular distribution for electrons from $e^{-}\gamma \to Ze^{-}, W^{-}\nu_e \to e^{-}\nu_e\overline{\nu_e}$.

resulting in a simultaneous efficiency loss. The energy spectrum for signal and background before and after cuts is shown in Figure 6.

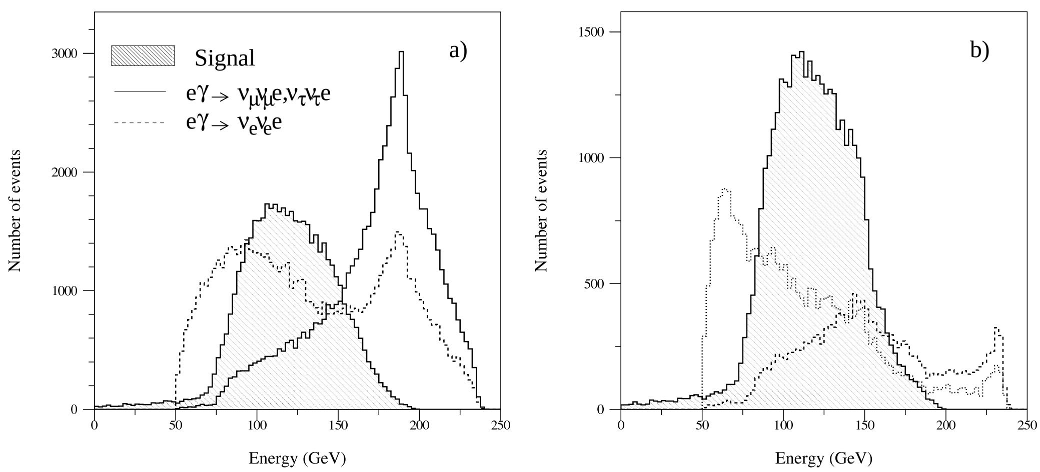

Figure 6: Energy distribution for signal and background events before (a) and after (b) cuts.

4 Selectron mass

For a fixed beam energy, the mass of the selectron and the neutralino can be measured from the endpoints of the electron energy distribution [5]. For a variable beam energy the endpoints are assumed for the maximum selectron energy, so that in principle they can still be used for the mass determination. The shape of the electron distribution gets largely diluted due to the variable beam energy and boost of the produced selectrons. If the photon spectrum is known, however, the endpoints can still be reconstructed from a fit to the electron energy spectrum.

It turns out the lower endpoint can be reconstructed fairly well, while the upper endpoint is affected much more by the background and the selectron boost. It is therefore not possible to reconstruct the selectron and neutralino mass with high precision. However, if the neutralino mass is known from e^+e^- running a good precision on the selectron mass is obtained.

For the measurement of the lower endpoint the background subtracted, falling part of the spectrum is fitted by a straight line and the intersect at zero is defined as the endpoint. To correct for possible biases a calibration curve has been generated (Fig. 7 left) and the mass of the selectron and its error for the reference sample is obtained comparing the fit result with the reference curve. For the studied parameter set and one year of running a measurement of

$$m(\tilde{e}_R^-) = 269.79 \pm 0.85\,\mathrm{GeV}$$

is possible, corresponding to a precision of 0.3%.

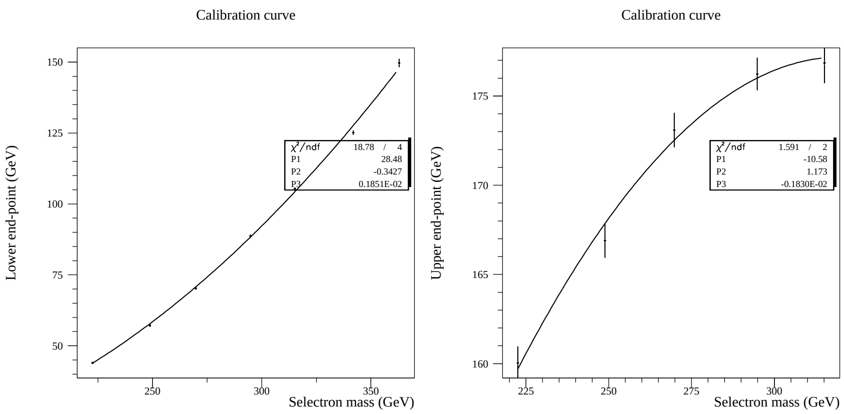

Figure 7: Calibration curve for the selectron mass determination from the lower endpoint of the electron momentum (left) and the upper endpoint of the transverse momentum (right).

A similar procedure has been tried with the upper endpoint. To overcome the problem with the boost the transverse momentum has been used instead of the momentum. However the corresponding calibration curve, not applying the p_t cut, is much flatter (Fig. 7 right) resulting in a significantly larger uncertainty of

$$m(\tilde{e}_R^-) = 269.8 \pm 6.1\,\mathrm{GeV},$$

corresponding to 2.3% uncertainty.

Up to now no systematic errors have been considered. The background can, however, be measured accurately using $W \to \mu\nu$ and visible Z decays. Especially the single W background, which is the largest one for the mass measurement from the lower endpoint, can be obtained with high statistical precision from a run with left-handed electron polarisation. Some uncertainties may come from the beam parameters like the energy spectrum and the polarisation which have to be quantified in a future study.

5 Conclusions

The scenario has been studied where gauginos are seen at an e^+e^- linear collider while the selectron is only visible in $e\gamma$ collisions. In this case the process $e^-\gamma \to \tilde{e}^-\tilde{\chi}_1^0$ can be separated cleanly from the background if the beams can be highly polarised. Within one year of running with right handed electrons and photons the selectron production cross section can be obtained with a statistical precision of 0.75% and the selectron mass can be measured with a statistical precision of around 0.3%.

References

[1] ECFA/DESY Photon Collider Working Group, B. Badelek *et al.*, TESLA Technical Design Report, Part VI, Chapter 1: Photon collider at TESLA, hep-ex/0108012, DESY-01-011E.

[2] T. Gleisberg, S. Hoche, F. Krauss, A. Schalicke, S. Schumann and J. C. Winter, JHEP **0402** (2004) 056 [arXiv:hep-ph/0311263].

[3] A. F. Zarnecki, *CompAZ: parametrization of the photon collider luminosity spectra*, LC-TOOL-2002-007.

[4] V. D. Barger, T. Han and J. Kelly, Phys. Lett. B **419** (1998) 233 [arXiv:hep-ph/9709366].

[5] H.U.Martyn, G.Blair, *Determination of sparticle masses and SUSY parameters*, LC-TH-2000-023